Factors Influencing the Kinetics of Esterification of Fatty Acids over Solid Acid Catalysts

ARTICLE · SEPTEMBER 2011

DOI: 10.1021/ef2009138

CITATIONS
12

READS
47

3 AUTHORS, INCLUDING:

Jitendra Satyarthi
Bharat Petroleum
21 PUBLICATIONS **248** CITATIONS
SEE PROFILE

Sambhu Radhakrishnan
University of Leuven
6 PUBLICATIONS **50** CITATIONS
SEE PROFILE

energy&fuels

ARTICLE

pubs.acs.org/EF

Factors Influencing the Kinetics of Esterification of Fatty Acids over Solid Acid Catalysts

Jitendra Kumar Satyarthi, Sambhu Radhakrishnan, and Darbha Srinivas*

Catalysis Division, National Chemical Laboratory, Pune 411 008, India

ABSTRACT: The kinetics of esterification of fatty acids with alcohols over three different solid acid catalysts, viz., large pore zeolite-β (Hβ), micro-mesoporous Fe−Zn double-metal cyanide (DMC), and mesoporous Al-MCM-41, have been reported. Hydrophobicity of these catalysts increases in the order: Al-MCM-41 < Hβ < DMC. The chain lengths of the fatty acid ($C_{8.0}$−$C_{18.1}$) and alcohol (C_1−C_8) molecules have been varied, and their influence on kinetic parameters has been studied. The present study reveals that porosity and surface hydrophobicity of the catalyst are the two important factors other than acid properties (concentration and strength of acid centers) that influence the esterification reaction.

1. INTRODUCTION

Biodiesel is a nontoxic, biodegradable, renewable fuel comprised of monomethyl or ethyl esters of long-chain fatty acids (FAMEs or FAEEs) derived from vegetable oils or animal fat by reaction with methanol or ethanol.[1−6] Biodiesel helps in reducing air pollution because it produces lower amounts of SO_x, CO_x, hydrocarbons (HCs), and particulate matter. Non-edible oils are sustainable feedstock for biodiesel production. However, these oils contain a significant amount of free fatty acids (FAs). Conventional base catalysts cannot be used for biodiesel production from non-edible oils because of saponification of these FAs by cations of the base.[5] Solid acids, which can catalyze simultaneously the esterification of FAs and transesterification of fatty acid glycerides into FAME/FAEE biodiesel, are considered as efficient catalysts for such low-grade, non-edible oil feedstocks.[7−11] Alternatively, a two-step process has to be adopted, wherein the FAs are esterified in the first step using an acid catalyst prior to transesterification of the triglycerides by a base catalyst.[12,13] Solid acid catalysts eliminate corrosion, environmental, and handling problems associated with the use of conventional mineral acid catalysts. An understanding of the factors influencing the esterification reaction is of great importance in designing more efficient solid acid catalysts. Steric and diffusional effects,[14] pore size of the catalysts,[15] and polarity of the acid chain[16] have been reported to play an important role on esterification and transesterification reactions of vegetable oils over solid catalysts. Recently, we had demonstrated that surface hydrophobicity of the catalyst and the relative adsorption of reactants/products are two additional parameters that influence the kinetics of esterification of long-chain FAs over solid catalysts.[17] This effect was shown using carboxylic acids with varying chain length ($C_{8.0}$−$C_{18.1}$) and catalysts with hydrophilic or hydrophobic surfaces. In this study, we report the influence of porosity by comparing the kinetic data of two chemically similar systems (Al-MCM-41 and Hβ) but differing in their pore dimensions. We also report the influence of the chain length of alcohol (C_1−C_8) molecules on the kinetics of the esterification reaction.

2. EXPERIMENTAL SECTION

2.1. Catalyst Preparation and Characterization. Large pore zeolite-β (Hβ) (SiO_2/Al_2O_3 = 28) was supplied by the Catalyst Pilot Plant, National Chemical Laboratory, Pune, India. Al-MCM-41 (SiO_2/Al_2O_3 = 96) and micro-mesoporous Fe−Zn double-metal cyanide (DMC) were prepared and characterized as reported by us earlier.[17]

2.2. Reaction Procedure. Esterification of FAs [octanoic acid ($C_{8.0}$), decanoic acid ($C_{10.0}$), dodecanoic acid ($C_{12.0}$), palmitic acid ($C_{16.0}$), and oleic acid ($C_{18.1}$)] with methanol was conducted in batch reactors over Hβ and Al-MCM-41 catalysts. In a typical reaction, 0.15 g of catalyst and 17.7 mmol of FAs and methanol (FA/methanol molar ratio = 1:10) were taken in a Teflon-lined, stainless-steel autoclave (100 mL). The reaction was conducted at a desired temperature for a desired period of time by mounting the autoclave in a rotating hydrothermal reactor (Hiro Co., Japan). At the end of reaction, the autoclave was cooled to 298 K and the catalyst was separated by filtration. Methanol from the reaction mixture was removed using a rotavapor. The acid values of the reaction mixture at the beginning and end of the reaction were determined by titration with 0.1 N NaOH solution. Phenolphthalein was used as an indicator.

2.3. Kinetic Parameters. The kinetic parameters were determined by carrying out the esterification reactions at similar conversion levels. For each fatty acid ($C_{8.0}$−$C_{18.1}$), the reactions were conducted at four different temperatures (363, 373, 383, and 393 K over Hβ and 393, 403, 413, and 423 K over Al-MCM-41). All of the experimental data points collected over 8 h were fitted to a curve passing through origin. From this curve (conversion versus time plot), initial rates were determined. These were then used to calculate the rate constant (k) using the pseudo-first-order rate law. Employing the Arrhenius equation and the k values determined at different temperatures, activation energy (E_a) values were determined.

Reactions were also investigated in a similar manner between oleic acid ($C_{18.1}$) and alcohols of varying chain length [methanol (C_1), ethanol (C_2), 1-propanol (C_3), 1-butanol (C_4), 1-pentanol (C_5), 1-hexanol (C_6), and 1-octanol (C_8)]. A total of 0.06 g of catalyst (Hβ, Al-MCM-41, or DMC) and 2 g of oleic acid and alcohol (FA/alcohol molar ratio = 1:10) were taken, and the kinetic data were determined.

2.4. ^{1}H Nuclear Magnetic Resonance (NMR) Method To Monitor the Esterification Reaction. FA conversion was independently estimated by ^{1}H NMR spectroscopy (Bruker AV, 200 MHz).[18] In this method, the sample was prepared by dissolving 20 mg of the

Received: August 20, 2010
Revised: August 2, 2011
Published: August 02, 2011

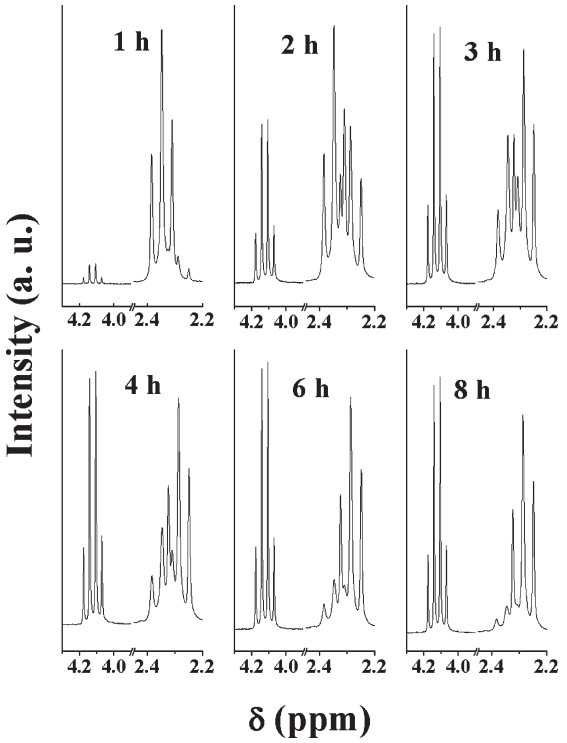

Figure 1. ^{1}H NMR spectra as a function of the reaction time: esterification of oleic acid with ethanol.

reaction mixture in 2 mL of $CDCl_3$ taken in a 5 mm (outer diameter) NMR tube. ^{1}H NMR spectra were recorded using the following conditions: pulse width, 13.4 μs; pulse delay, 1 s; spectral width, 4136.2 Hz; data points, 16 384; and number of scans, 32. The method of estimation is as follows. Consider oleic acid and its ethyl ester.

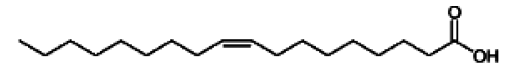

Oleic acid

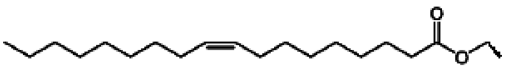

Ethyl oleate

In general, the α-CH_2 groups of oleic acid and ethyl oleate show ^{1}H NMR signals (triplet) in the chemical shift (δ) range of 2.4−2.2 ppm (Figure 1). However, the triplet corresponding to oleic acid occurs at a slightly higher δ value than that of ethyl oleate because of the greater deshielding by the carboxylic group compared to the ester group. When both acid and ester are present in the sample, the spectrum looks like a multiplet pattern because of overlapping of the α-CH_2 triplet signals of ester and acid molecules. The −CH_2 of the ethoxy group of ethyl oleate shows a quartet in the δ range of 4.2−4.0 ppm (Figure 1). As the esterification reaction progresses, the intensity of the signals at 4.2−4.0 ppm increases, while the overall area of the multiplet peaks at δ 2.4−2.2 remains the same (Figure 1). Acid conversion can be estimated by comparing the areas of these signals because of α-CH_2 (δ 2.4−2.2) and −CH_2 of the ethoxy part of ethyl oleate (δ 4.2−4.0), as defined by the equation given below

$$\text{fatty acid conversion (\%)} = \frac{A_{CH_2(\text{ethoxy})}}{A_{\alpha\text{-}CH_2(\text{total})}} \times 100$$

where $A_{CH_2(\text{ethoxy})}$ is the area of methylene protons of the ethoxy group in the ester and $A_{\alpha\text{-}CH_2(\text{total})}$ is the total area of α-CH_2 signals of acid and ester,

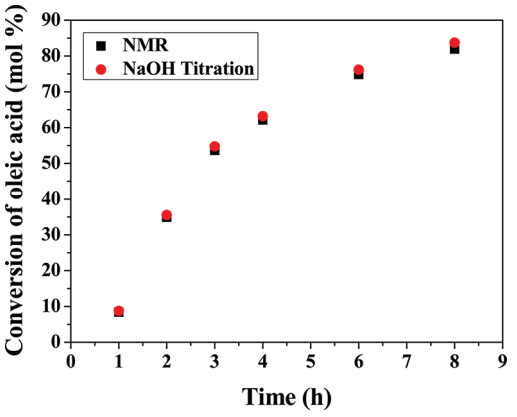

Figure 2. Oleic acid conversion estimated independently by ^{1}H NMR and alkali titration.

respectively. While a similar expression is valid for esterification with other long-chain alcohols used in this study, the following equation is used for the reactions with methanol. The factors 2 and 3 in this equation arise because of the fact that the α-CH_2 group contains two protons, while the methoxy group in the methyl ester contains three protons. The conversions determined by ^{1}H NMR and titration methods are in good agreement with each other (Figure 2).

$$\text{fatty acid conversion (\%)} = \frac{2A_{CH_3(\text{methoxy})}}{3A_{\alpha\text{-}CH_2(\text{total})}} \times 100$$

3. RESULTS AND DISCUSSION

3.1. Physicochemical Characterization. Table 1 lists the surface and acidic properties of Hβ, Al-MCM-41, and DMC catalysts. Detailed characterization of the catalysts was reported elsewhere.[13,17,19] Al-MCM-41 is an ordered mesoporous material (average pore diameter is 3.6 nm), while Hβ is microporous (average pore diameter is 0.7 nm). As revealed by N_2 physisorption and high-resolution transmission electron microscopic studies, DMC is mostly microporous but also contains some mesopores in its architecture (average pore diameter is 2.5 nm). The specific surface area of these catalysts decreases in the order: Al-MCM-41 (642 m^2/g) > Hβ (577 m^2/g) > DMC (52 m^2/g). The acidic properties of the catalysts were determined using NH_3 and pyridine as probe molecules. Representative temperature-programmed desorption of ammonia (NH_3-TPD) profiles and diffuse reflectance infrared Fourier transform (DRIFT) spectra of adsorbed pyridine of Al-MCM-41 and Hβ are shown in Figure 3. The infrared (IR) peaks at 1640 and 1544 cm^{-1} in the case of Al-MCM-41 and at 1620 and 1542 cm^{-1} in the case of Hβ are due to Brönsted acid (B) sites (right panel of Figure 3). The peaks at 1595 and 1445 cm^{-1} for Al-MCM-41 and 1592 and 1439 cm^{-1} for Hβ are due to Lewis acid (L) sites. The peaks at 1490 cm^{-1} (for Al-MCM-41) and 1486 cm^{-1} (for Hβ) correspond to both B and L sites. On the basis of the area of IR peaks at 1542−1544 cm^{-1} (for B sites) and 1439−1445 cm^{-1} (for L sites) and using molar extinction coefficients reported by Emeis,[20] the ratio of L/B was estimated to be 8.4 and 1.9 for Hβ and Al-MCM-41, respectively. Both Al-MCM-41 and Hβ showed two broad NH_3 desorption peaks in the temperature range of 400−950 K (left panel of Figure 3). The position of these peaks occurred at a higher temperature in the case of Al-MCM-41 (555 K) than in Hβ (476 K). However, the total acidity

dx.doi.org/10.1021/ef2009138 |*Energy Fuels* 2011, 25, 4106–4112

Table 1. Surface and Acidic Properties of Solid Acid Catalysts

property	catalyst		
	Al-MCM-41	Hβ	DMC
specific surface area (S_{BET}, m^2/g)	642	577	52
average pore diameter (nm)	3.6	0.7	2.5
pore volume (cm^3/g)	0.58	0.39	0.01
pore type	mesoporous	micoporous	microporous and some mesoporosity
particle size (SEM, μm)	1.0	0.7	1.4
surface structure	hydrophilic	hydrophilic	hydrophobic
acidity (NH_3-TPD, mmol/g)	0.24	0.68	0.84
acid type	Lewis and Brönsted	Lewis and Brönsted	Lewis

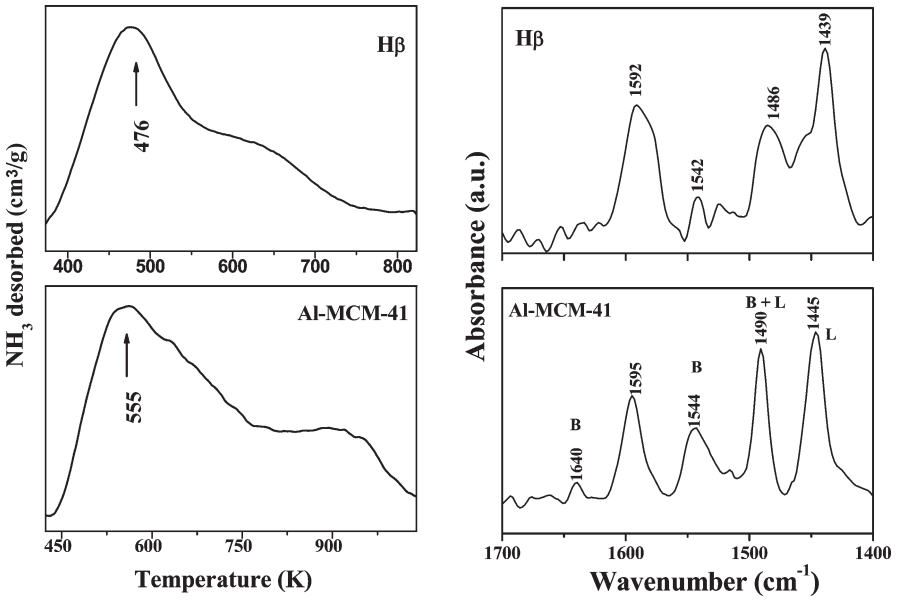

Figure 3. (Left) NH_3-TPD profiles. (Right) DRIFT spectra of adsorbed pyridine.

of Hβ (NH_3-TPD) was found to be higher (0.68 mmol/g) than that of Al-MCM-41 (0.24 mmol/g), which agrees well with the Al content of these catalysts. DMC contains only the Lewis acid sites (0.84 mmol/g).[17]

3.2. Catalytic Activity: Esterification of Fatty Acids with Methanol. With a view to demonstrate the effect of pore architecture on kinetic parameters for esterification of long-chain fatty acids, Hβ and Al-MCM-41 were chosen as the catalysts of choice. These two catalysts are chemically similar but differ in their porosity. While Al-MCM-41 is mesoporous, Hβ is a microporous catalyst. Al-MCM-41 has a two-dimensional (hexagonal symmetry) pore architecture, whereas Hβ has an ordered three-dimensional structure.

In kinetic studies, methanol was taken in excess of FAs (10 times), so that the reaction follows a pseudo-first-order rate law. Although we have used the simple and most popular pseudo-homogeneous model, it should be noted that there are multiple elementary steps, including adsorption, reaction, and desorption of species, which all contribute to the overall kinetics. Figure 4 shows the conversion versus time plots in the esterification of fatty acids of varying chain length ($C_{8.0}$−$C_{18.1}$) with methanol at 423 K and in the reaction of oleic acid with methanol at different temperatures (363−393 K) over the Hβ catalyst. The plot of ln k versus $1/T$ is linear, and a satisfactory fit between experimental points and the theoretical line was obtained (Figure 4). The kinetic data [rate constant (k) and activation energy (E_a)] estimated from these plots are listed in Table 2. The following observations can be made from Table 2: (i) In general, the rate parameters [rate constant (k) and turnover frequency (TOF; moles of FA converted per mole of Brönsted + Lewis acid sites per second)] are higher for Al-MCM-41 than for Hβ. (ii) They (k and TOF) increased with an increase in the chain length of FA. (iii) $C_{18.1}$ deviated from this relationship. Its values are smaller than those of $C_{16.0}$. While $C_{18.1}$ is an unsaturated FA (double bond is present between the 9th and 10th carbon atoms in the fatty acid chain), the rest of the acids are saturated. This difference in the chemical structure of FAs is perhaps the cause for the difference in the expected variation in rate parameters. (iv) In general, activation energy (E_a) values increased with an increase in the chain length of FAs. (v) The E_a values for shorter chain length fatty acids ($C_{8.0}$ and $C_{10.0}$) are nearly the same for both Hβ and Al-MCM-41. However, the difference increased with an increase in the chain length of FAs.

Despite a higher acid concentration, the kinetic parameters of Hβ are smaller than those of Al-MCM-41 (Table 2). If acidity alone is the controlling factor, then one should have

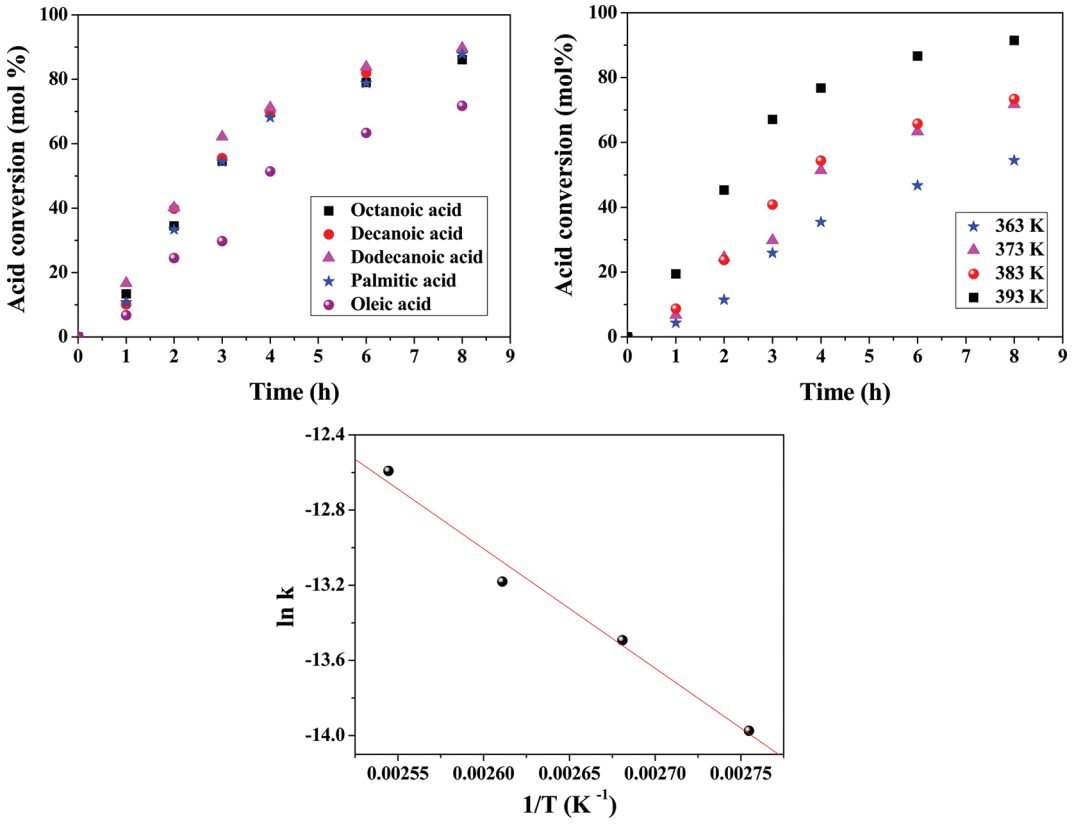

Figure 4. Kinetic studies over the Hβ catalyst: (top-left panel) esterification of different FAs with methanol at 373 K, (top-right panel) esterification of oleic acid with methanol at different temperatures, and (bottom panel) Arrhenius plot for the oleic acid−methanol system.

Table 2. Kinetic Parameters for Esterification of Fatty Acids with Methanol over Hβ and Al-MCM-41[a]

	Al-MCM-41				Hβ			
fatty acid	T	k ($\times 10^{-8}$)	TOF ($\times 10^{-3}$)	E_a	T	k ($\times 10^{-8}$)	TOF ($\times 10^{-3}$)	E_a
octanoic acid ($C_{8.0}$)	393	1.9	6.9	24.1	363	1.0	3.2	24.7
	403	3.3	8.3		373	1.4	6.4	
	413	4.3	16.0		383	2.4	8.4	
	423	4.7	12.2		393			
decanoic acid ($C_{10.0}$)	393	1.9	11.1	29.4	363	0.9	4.7	26.9
	403	3.1	19.7		373	1.0	4.9	
	413	4.1	19.7		383	1.4	8.4	
	423		21.3		393	2.2		
dodecanoic acid ($C_{12.0}$)	403	3.5	18.3	25.3	363	2.2	5.4	34.7
	413	4.9	29.9		373	3.5	7.8	
	423		29.1		383	3.9	9.4	
palmitic acid ($C_{16.0}$)	433	6.0	39.1	37.9	393	5.6		46.0
	403	6.3	27.8		373	2.1	5.2	
	413	6.2	36.3		383	3.7	9.1	
	423	6.8	49.9		393	4.7		
	433	10.4	44.2		403	6.5		
oleic acid ($C_{18.1}$)	403	4.2	18.3	38.9	363	1.0	2.1	54.7
	413	6.2	20.2		373	1.6	3.3	
	423	6.9	26.9		383	1.6	4.2	
	433	9.9	43.2		393	3.9	9.4	

[a] The rate constant (k) is represented in units of L mol^{-1} s^{-1} m^{-2}; the activation energy (E_a) is represented in units of kJ mol^{-1}; and the temperature (T) is represented in kelvin. The turnover frequency (TOF, s^{-1}) is moles of fatty acid converted per mole of (Brönsted + Lewis) acid sites on the catalyst per second. Data for Al-MCM-41 are from our earlier report.[17]

dx.doi.org/10.1021/ef2009138 |*Energy Fuels* 2011, 25, 4106–4112

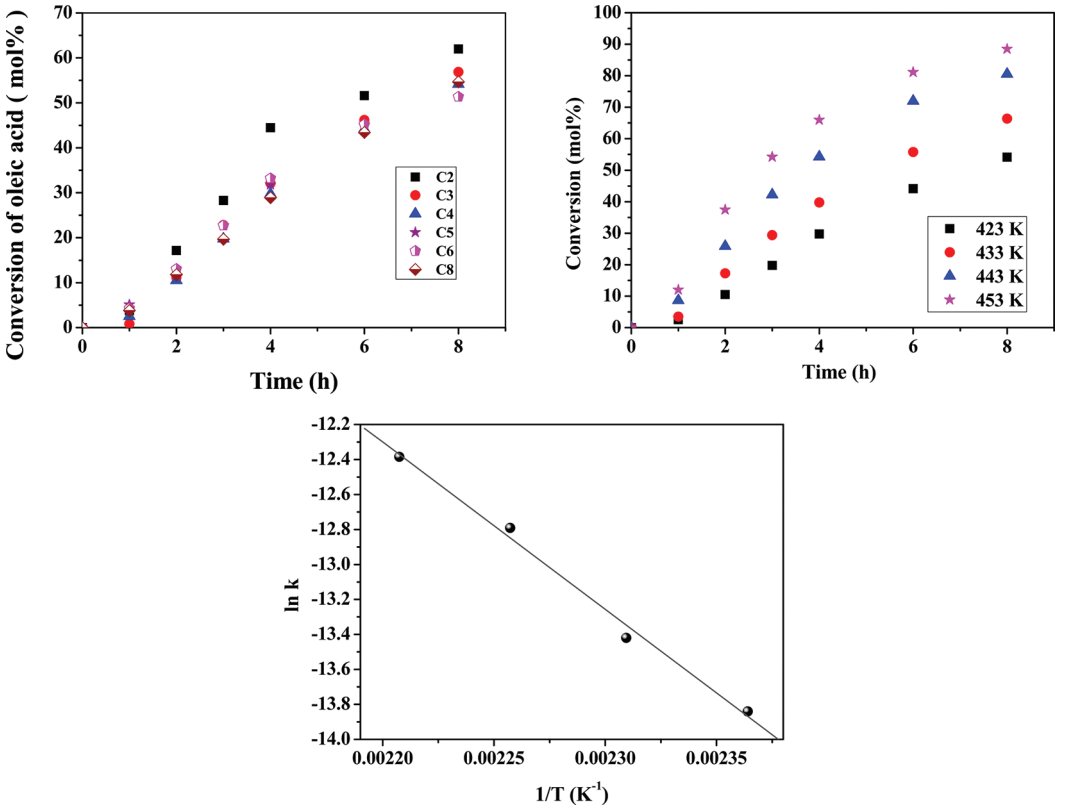

Figure 5. (Top-left panel) Fatty acid conversion versus time plots for esterification of oleic acid with different alcohols at 423 K. (Top-right panel) Fatty acid conversion versus time plots for esterification of oleic acid with 1-butanol at different temperatures. (Bottom panel) Arrhenius plot for esterification of oleic acid with 1-butanol. Catalyst = DMC.

observed a reverse trend. As stated above, the activation energy increased with the chain length of FAs (Table 2). However, the extent of the increase in E_a values is lower for two-dimensional, mesoporous Al-MCM-41 than for microprous Hβ zeolite. All of these observations indicate the importance of the pore size and pore-dimensionality effects on the kinetic parameters. Because transport is associated with the bending and wiggling of the molecules, its activation energy ought to be much smaller (e.g., a few kJ/mol) than that of chemical reaction rates. Indeed, classically, the apparent activation energy of transport-limited processes is smaller than that of kinetically limited processes. The much larger differences in activation energy especially in the case of long-chain length fatty acids do indicate that additional factors (hydrophobicity and adsorption−desorption rates of reactants, for example) apart from pore architecture are also influencing the activation energy parameter. Further, from the inspection of turnover frequencies, it appears that there may be a gradient in the number and activity of the acid sites in the catalysts of the present study. The smaller molecules can readily access more of the acid sites than the larger molecules. NH_3-TPD studies (left panel of Figure 3) showed the desorption peaks at higher temperatures for Al-MCM-41 than for Hβ, indicating that the strength of acid centers is higher in the case of the former than in the latter catalyst. This higher strength of acid centers would have also contributed to the more efficient activity of Al-MCM-41 than Hβ.

The activation energy for esterification of palmitic acid with methanol over Hβ and Al-MCM-41 is higher (46.0 and 37.9 kJ/mol, respectively) than for homogeneous sulfuric acid and methanesulfonic acid catalysts (27.3 and 15.8 kJ/mol, respectively).[21] This difference, in the case of solid catalysts, is due to diffusional limitations in the pores and surface effects. However, the rate constant and activation energy values of Hβ and Al-MCM-41 are comparable to those of various commercial solid acid catalysts.[17,22]

3.3. Catalytic Activity: Esterification of Oleic Acid with Alcohol of Varying Chain Length. Oleic acid was esterified with methanol (C_1), ethanol (C_2), 1-propanol (C_3), 1-butanol (C_4), 1-pentanol (C_5), 1-hexanol (C_6), and 1-octanol (C_8). Each reaction was conducted at four different temperatures for 1−8 h over Hβ, Al-MCM-41, and DMC catalysts. As in the above experiments, alcohol was taken in excess (10 times), so that a pseudo-first-order rate law is obeyed. Figure 5 shows representative kinetic plots obtained over the DMC catalyst. The kinetic data (k and TOF) and energy of activation (E_a) for all of the three catalysts are compiled in Table 3.

Even in these experiments, the kinetic parameters of Al-MCM-41 are higher than those of Hβ. The values of DMC (micro-mesoporous material) are higher than both Hβ and Al-MCM-41. While an increase in the value of k with an increase in the chain length of alcohol was observed over DMC, no systematic variation was found with Al-MCM-41 and Hβ catalysts. The variation in E_a with the chain length of alcohols is different over each catalyst (Figure 6). Over Al-MCM-41, the value of E_a increased slowly from methanol to 1-butanol and then steeply from 1-butanol to 1-octanol. In the case of Hβ, the E_a values decreased with an increase in the chain length of alcohol. This

dx.doi.org/10.1021/ef2009138 |*Energy Fuels* 2011, 25, 4106–4112

Table 3. Esterification of Oleic Acid with Different Alcohols[a]

	DMC				Al-MCM-41				Hβ			
alcohol	T	k ($\times 10^{-7}$)	TOF ($\times 10^{-3}$)	E_a	T	k ($\times 10^{-8}$)	TOF ($\times 10^{-3}$)	E_a	T	k ($\times 10^{-8}$)	TOF ($\times 10^{-3}$)	E_a
methanol	423	4.2	3.8	52.8	403	10.4	18.3	38.9	363	2.5	2.1	54.7
	433	4.3	4.1		413	15.6	20.2		373	4.0	3.3	
	443	8.1	6.7		423	17.2	26.9		383	3.9	4.2	
	453	11.5	9.9		433	24.7	43.2		393	9.8	9.4	
ethanol	423	3.7	1.5	54.7	393	0.9	21.6	40.8	373	0.5	3.7	49.9
	433	5.7	2.6		403	1.6	36.6		383	1.4	9.6	
	443	7.8	3.4		413	2.0	55.4		393	1.9	14.8	
	453	10.3	4.4		423	2.9	76.8		403	2.6	15.8	
1-propanol	423	4.0	0.3	57.1	393	1.0	19.0	38.7	373	1.1	3.1	28.2
	433	5.2	1.1		403	1.2	31.6		383	1.3	5.7	
	443	6.7	3.2		413	1.6	38.0		393	1.1	8.5	
	453	11.6	4.1		423	2.4	56.5		403	2.1	11.8	
1-butanol	423	4.2	1.0	61.5	393	1.1	9.2	38.4	373	0.9	3.7	22.4
	433	5.3	1.4		403	1.4	20.8		383	1.1		
	443	12.2	3.4		413	1.9	28.1		393	1.1	4.9	
	453	12.6	4.7		423	1.8	47.4		403	1.9	6.5	
1-pentanol	423	5.0	2.0	53.0	403	3.2	33.5	42.1	383	1.0	4.3	28.4
	433	8.4	2.5		413	3.5	39.3		393	1.2	5.7	
	443	11.3	3.0		423	5.8	53.4		403	1.6	9.6	
	453	13.5	3.6		433	6.3	80.6		413	2.7	15.4	
1-hexanol	423	5.9	1.7	46.8	403	2.6	30.9	54.3	383	0.7	3.9	21.2
	433	9.0	3.1		413	4.5	41.9		393	2.0	5.2	
	443	12.2	3.7		423	6.8	56.7		403	2.2	9.6	
	453	14.1	4.4		433	7.8	77.7		413	2.7	13.7	
1-octanol	423	7.0	1.5	43.8	403	1.9	30.3	55.9	383	2.1	4.8	24.0
	433	10.8	2.5		413	2.1	41.7		393	2.3	6.8	
	443	13.8	3.0		423	2.9	60.8		403	3.2	7.6	
	453	16.0	3.6		433	3.2	76.3		413	3.6	13.7	

[a] The rate constant (k) is represented in units of L mol^{-1} s^{-1} m^{-2}; the activation energy (E_a) is represented in units of kJ mol^{-1}; and the temperature (T) is represented in kelvin. The turnover frequency (TOF, s^{-1}) is moles of fatty acid converted per mole of (Brönsted + Lewis) acid sites on the catalyst per second.

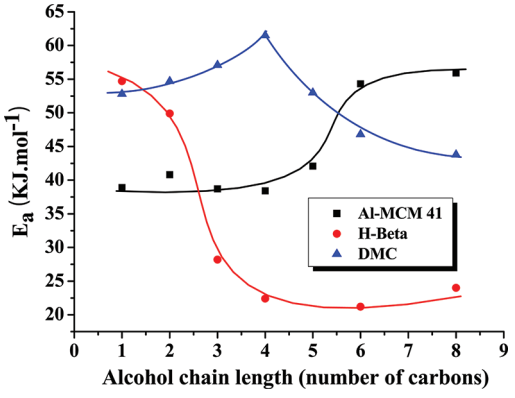

Figure 6. Variation in energy of activation (E_a) with the chain length of alcohols in the esterification of oleic acid over different solid acid catalysts.

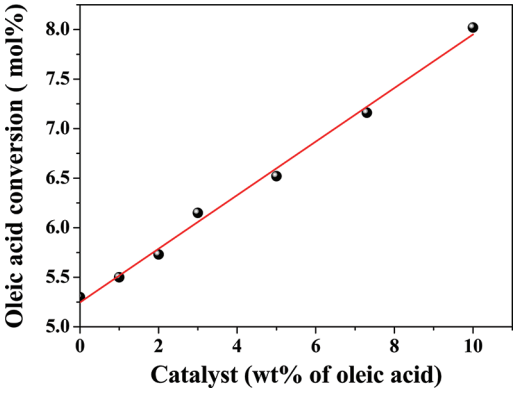

Figure 7. Influence of the amount of catalyst: esterification of oleic acid with methanol (reaction conditions: catalyst, DMC; acid, 7.08 mmol; acid/methanol molar ratio, 1:1; temperature, 423 K; and time, 1 h).

decrease is, however, more noticeable up to 1-butanol. Over DMC, the value of E_a increased with an increasing chain length of alcohol up to 1-butanol and then decreased beyond that. These behaviors can be explained in terms of the influence of the pore structure and surface hydrophobicity of the catalysts. In the reactions of oleic acid with alcohols, the addition to the double bond may occur[23] and also a double bond shift might take place. However, we did not observe these side reactions at our experimental conditions.

dx.doi.org/10.1021/ef2009138 |*Energy Fuels* 2011, 25, 4106–4112

In all of these studies, miscibility of reactants is not an issue. All of the alcohols including methanol are completely miscible with fatty acids even at room temperature. By varying the active-site density within a given catalyst particle, Madon and Boudart[24] proposed that, if the rate per active-site density is constant (at two different temperatures), then the rate is free from transport artifacts. In the present study, we have changed the amount of catalyst loaded from 1 to 10 wt % and estimated the conversion. As seen from Figure 7, for DMC, at 423 K, for the reaction of oleic acid with methanol, the acid conversion increased proportionally with the amount of catalyst, indicating that there is no mass-transfer limitation in this experiment.

Diffusion of oleic acid and alcohols into the pores of Al-MCM-41 should not be an issue because this catalyst is mesoporous in nature (average pore size = 3.6 nm). However, the pK_a of alcohols increases with an increase in the chain length. As a consequence of this, long-chain alcohols are more nucleophilic and, thereby, exhibit lower conversion and a higher E_a value. This behavior is observed up to 1-butanol. For higher alcohols, pK_a remains the same but their hydrophobicity keeps increasing. In an earlier study,[13,17] we had demonstrated that hydrophobicity of these solid catalysts decreases in the order: DMC > Hβ > Al-MCM-41. Hence, Al-MCM-41, having a hydrophilic surface, is expected to show higher E_a values with an increasing chain length of alcohols because of less adsorption of those molecules. In the case of microporous Hβ, with methanol as alcohol, the reaction might be taking place both inside the pores and on the external surface. As the chain length of alcohol increases, contribution of the reaction occurring inside the pore decreases and that at the external surface increases. This variation as well as its hydrophobic nature (compared to Al-MCM-41) is possibly the cause for the low E_a values in reactions with long-chain length alcohols. DMC has a hydrophobic surface structure with intermediate pore sizes (average pore diameter = 2.5 nm). The initial increase in E_a (from methanol to 1-butanol) is due to the increase in pK_a of the alcohol, and the latter decrease (beyond 1-butanol) is due to the increased adsorption of hydrophobic (higher) alcohols on the hydrophobic DMC surface. Generally, an increase in E_a values with alcohol chain length was reported by other researchers.[25,26] Those studies were made only with C_1-C_4 alcohols. Variation in the properties of catalysts and chain length of alcohols as well as acids enabled us, for the first time, to demonstrate that the pore size and hydrophobicity of the catalyst surface are the two additional important parameters that influence the fatty acid esterification reaction. On the basis of the results reported here, it can be concluded that the rate of esterification of long-chain fatty acids with alcohols can be enhanced by designing catalysts with large pore sizes, high acid strengths, and hydrophobic surface structure.

4. CONCLUSION

Esterification of fatty acids with alcohols was investigated over Hβ, Al-MCM-41, and Fe−Zn DMC catalysts. The chain lengths of fatty acids ($C_{8.0}-C_{18.1}$) and alcohol (C_1-C_8) were varied, and the kinetic parameters were determined. The studies revealed that porosity and surface hydrophobicity of the catalyst are the important parameters other than surface area and acidic properties (concentration and strength of acid centers) that influence the kinetics of the esterification reaction. The influence of porosity on kinetic parameters was demonstrated using Hβ and Al-MCM-41, which are chemically similar but differ in their porosity.

AUTHOR INFORMATION

Corresponding Author

*Telephone: +91-20-2590-2018. Fax: +91-20-2590-2633. E-mail: d.srinivas@ncl.res.in.

ACKNOWLEDGMENT

Jitendra Kumar Satyarthi acknowledges the Council of Scientific and Industrial Research (CSIR), New Delhi, India, for the award of a senior research fellowship.

REFERENCES

(1) Di Serio, M.; Tesser, R.; Pengmei, L.; Santacesaria, E. *Energy Fuels* **2007**, *22*, 207–217.
(2) Kiss, A. A.; Dimian, A. C.; Rothenberg, G. *Adv. Synth. Catal.* **2006**, *348*, 75–81.
(3) Helwani, Z.; Othman, M. R.; Aziz, N.; Kim, J.; Fernando, W. J. N. *Appl. Catal., A* **2009**, *363*, 1–10.
(4) Pinto, A. C.; Guarieiro, L. L. N.; Rezende, M. J. C.; Ribeiro, N. M.; Torres, E. A.; Lopes, W. A.; Pereira, P. A. P.; de Andrade, J. B. *J. Braz. Chem. Soc.* **2005**, *16*, 1313–1330.
(5) Ma, F. R.; Hanna, M. A. *Bioresour. Technol.* **1999**, *70*, 1–15.
(6) Schuchardt, U.; Sercheli, R.; Vargas, R. M. *J. Braz. Chem. Soc.* **1998**, *9*, 199–210.
(7) Sreeprasanth, P. S.; Srivastava, R.; Srinivas, D.; Ratnasamy, P. *Appl. Catal., A* **2006**, *314*, 148–159.
(8) Rattanaphra, D.; Harvey, A.; Srinophakum, P. *Top. Catal.* **2010**, *53*, 773–782.
(9) Suwannakarn, K.; Lotero, E.; Ngaosuwan, K.; Goodwin, J. G., Jr. *Ind. Eng. Chem. Res.* **2009**, *48*, 2810–2818.
(10) Yan, S. L.; Salley, S. O.; Ng, K. Y. S. *Appl. Catal., A* **2009**, *353*, 203–212.
(11) Lopez, D. E.; Goodwin, J. G., Jr.; Bruce, D. A.; Furuta, S. *Appl. Catal., A* **2008**, *339*, 76–83.
(12) Helwani, Z.; Othman, M. R.; Aziz, N.; Fernando, W. J. N.; Kim, J. *Fuel Process. Technol.* **2009**, *90*, 1502–1514.
(13) Satyarthi, J. K.; Srinivas, D.; Ratnasamy, P. *Appl. Catal., A* **2011**, *391*, 427–435.
(14) Liu, Y.; Lotero, E.; Goodwin, J. G., Jr. *J. Catal.* **2006**, *243*, 221–228.
(15) Mbaraka, I. K.; Radu, D. R.; Lin, V. S.-Y.; Shanks, B. H. *J. Catal.* **2003**, *219*, 329–336.
(16) Alonso, D. M.; Granados, M. L.; Mariscal, R.; Douhal, A. *J. Catal.* **2009**, *262*, 18–26.
(17) Satyarthi, J. K.; Srinivas, D.; Ratnasamy, P. *Energy Fuels* **2010**, *24*, 2154–2161.
(18) Satyarthi, J. K.; Srinivas, D.; Ratnasamy, P. *Energy Fuels* **2009**, *23*, 2273–2277.
(19) Higgins, J. B.; Lapierre, R. B.; Schlenker, J. L.; Rohrman, A. C.; Wood, J. D.; Kerr, G. T.; Rohrbaugh, W. J. *Zeolites* **1988**, *8*, 446–452.
(20) Emeis, C. A. *J. Catal.* **1993**, *141*, 347–354.
(21) Aranda, D. A. G.; Santos, R. T. P.; Tapanes, N. C. O.; Ramos, A. D.; Antunes, O. A. C. *Catal. Lett.* **2008**, *122*, 20–25.
(22) Peters, T. A.; Benes, N. E.; Holmen, A.; Keurentjes, J. T. F. *Appl. Catal., A* **2006**, *297*, 182–188.
(23) Lansalot-Matras, C.; Lozano, P.; Pioch, D.; Finiels, A.; Moreau, C.; Claude, S. *J. Am. Oil Chem. Soc.* **2006**, *83*, 725–729.
(24) Madon, R. J.; Boudart, M. *Ind. Eng. Chem. Fundam.* **1982**, *21*, 438–447.
(25) Srilatha, K.; Lingaiah, N.; Sai Prasad, P. S.; Prabhavathi Devi, B. L. A.; Prasad, R. B. N.; Venkateswar, S. *Ind. Eng. Chem. Res.* **2008**, *48*, 10816–10819.
(26) Lilja, J.; Murzin, D. Y.; Salmi, T.; Aumo, J.; Mäki-Arvela, P.; Sundell, M. *J. Mol. Catal. A: Chem.* **2002**, *182−183*, 555–563.